



HAL
open science

AMORPHOUS METALS AND γ -FE

U. Gonser

► **To cite this version:**

U. Gonser. AMORPHOUS METALS AND γ -FE. Journal de Physique Colloques, 1980, 41 (C1), pp.C1-51-C1-58. 10.1051/jphyscol:1980109 . jpa-00219579

HAL Id: jpa-00219579

<https://hal.science/jpa-00219579>

Submitted on 4 Feb 2008

HAL is a multi-disciplinary open access archive for the deposit and dissemination of scientific research documents, whether they are published or not. The documents may come from teaching and research institutions in France or abroad, or from public or private research centers.

L'archive ouverte pluridisciplinaire **HAL**, est destinée au dépôt et à la diffusion de documents scientifiques de niveau recherche, publiés ou non, émanant des établissements d'enseignement et de recherche français ou étrangers, des laboratoires publics ou privés.

AMORPHOUS METALS AND γ -Fe

U. Gonser

Angewandte Physik, Universität des Saarlandes, 6600 Saarbrücken, W-Germany

Abstract.- In recent years two aspects of physical metallurgy have attracted considerable interest from a scientific as well as from a technological point of view: amorphous metals of the $T_{80}M_{20}$ type ($T \rightarrow$ metal, $M \rightarrow$ metalloid) and the magnetic structure of γ -Fe.

I. Amorphous metals

1. Introduction.- The word "amorphous" is already causing a problem because some authors claim "glass" should be used instead. The question arises: what is the structure of these materials and which term best describes these alloys? The controversy is also apparent in the producer's trade names for these alloys: Metglas[®] (USA), Amomet[®] (Japan), Vitrovac[®] (Germany). It is interesting to note that in recent years the use of the term "amorphous" has given way more and more to "glass". Contributing factors in this development were the availability of the commercial Metglas[®] and the fact that for scientists and technologists "glass" sounds more interesting and more understood than amorphous.

The Greek origin of the word "amorphous" means lacking structure and form. Amorphous metals definitely have a structure - as a matter of fact, to find the nature of the structure is the basic motivation for

red as being released from the ill-defined amorphous pool (Fig.1). At present the term "amorphous metals" seems appropriate because it reflects the state of the art. In due time we will have a deeper understanding and well defined expressions will be coined. Specifically, if for the amorphous metals the micro-crystalline state can be ruled out and they are indeed liquid-like or can be represented by a random dense packing (RDP) we might use the designative "Bernal glass" or "metallic glass" or "metglass". In connection with the various controversies in the field of amorphous metals one might quote a recent article on "Science and Halfism": "When the importance of any particular issue emerged, it invariably has led to the development of polarized opinion, each opinion as extreme and fanatical as the other in its absolute conviction. At first, one camp would appear to have the day, only to be later superceded by the other. The irony of this haggling over opposite views has been that the final resolution of the issue has recognized that the truth of the matter seemed to lie somewhere, usually halfway, between the two extremes"¹. Amorphous films consisting of metals such as Sn, Bi, Pb, were first obtained in the 1950's by vapor quenching techniques involving condensation on cold substrates². However, the stability ranges of these films are rather limited and crystallization occurs at temperatures below 100 K. In the following years a large variety of

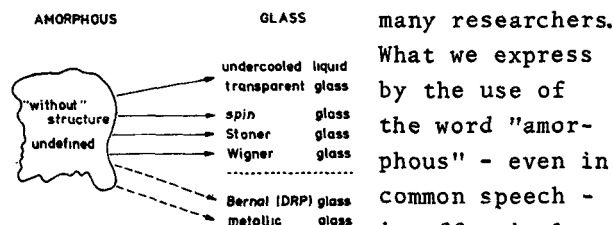
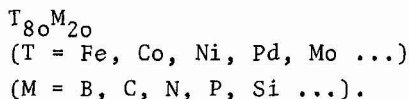


Fig.1: Amorphous vs. glass our ignorance or inability to define anything. In contrast glasses are usually defined: transparent glasses as undercooled liquids, for instance, or spin glasses, Wigner glasses, Stoner glasses etc. Glasses might be consid-

amorphous metals was produced by rapid quenching techniques³⁻⁶, after it was found that the amorphous state can be stabilized significantly by alloying with high valence elements of small size, which are known to occupy interstitial lattice sites in metals and exhibit covalent bonding in their elementary states. In general the composition range of the relatively stable amorphous state is found in the vicinity of 80 at % metal and 20 at % metalloid:



In recent years, one has learned to produce these amorphous materials in continuous processes and thus in large quantities. In addition, they can be "tailor made" for specific applications by varying the compositions and processing procedures. This technological development was accompanied by an increasing scientific interest and a desire to understand the nature of the amorphous metals. Naturally, something which seems to lack structure is a challenge to scientists. Another reason for the popularity of this field is that these materials are ideally suitable for modern man's favorite game - playing with the computer. The amorphous state is most inviting as a play ground for anyone interested in building up structures from "balls" by computer simulation.

The great scientific interest is demonstrated by the increasing number of conferences on this topic and the avalanche of books and publications in this field estimated to be close to 3000, of which about 100 apply Mössbauer spectroscopy to these materials. Due to lack of space only a few could be listed in the references⁷⁻¹⁴. Here we restrict ourself to the $T_{80}M_{20}$ type. But it should be noted that our Mössbauer conferences have covered the other types of amorphous materials rather well in previous invited talks. Of particular interest in this connection is last years' talk by J. Chappert¹⁵ on amorphous magnetic rare earth alloys.

2. Properties of $T_{80}M_{20}$ Alloys.- Extraordinarily deep eutectics are found, which already indicates a certain stability. As an example the Fe-B phase diagram¹⁶ is shown in Fig.2. The densities of these alloys are relatively large and the change in their volumes compared to the melt is only a few tenths of a percent. Their high electrical resistivities ρ are comparable to those of liquid metals and the change in ρ over several hundred degrees of temperature is usually only a few percent. The resistance to corrosion of these alloys is also significant. The magnetic properties of amorphous metals are of special interest to technology because they combine magnetic softness (low coercive forces and high permeability) with high mechanical strength and extreme hardness.

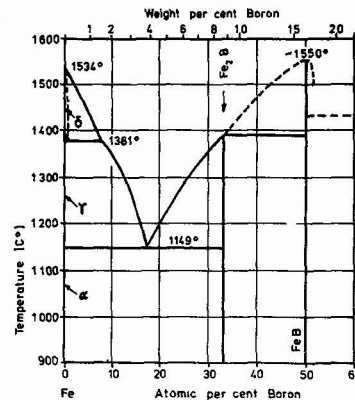
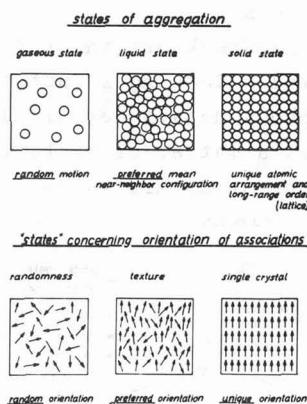


Fig.2: Fe-B phase diagram

over several hundred degrees of temperature is usually only a few percent. The resistance to corrosion of these alloys is also significant. The magnetic properties of amorphous metals are of special interest to technology because they combine magnetic softness (low coercive forces and high permeability) with high mechanical strength and extreme hardness.

3. Structure.- Controversy persists as to the nature of the short-range atomic arrangement. Considering the three states of aggregation schematically shown in Fig.3

(top) one might ask the question: are the amorphous metals more closely related to an undercooled liquid with some kind of continuous random structure or do they consist of small units - small crystallites of borides, carbides, nitrides etc. Fig.3:



with unique atomic arrangements - separated from each other by "grain boundaries". Or is the quenched-in structure already the first stage according to the Ostwald rule¹⁷? At present the main controversy is: random structure versus micro- or quasi-

crystallites or "molecules". However, one should realize that scientists too often depend on idealized models. On this specific issue the two points of view move closer together if on the one side a certain deviation from randomness is allowed, and on the other side the micro- and quasi-crystallites or molecules are redefined in terms of size, symmetry, orientation, stoichiometry etc. In other words, the problem is to find the dividing line between the definitions of the "molecules" with a fixed structure¹⁸, the "quasi-crystallites based on a locally distorted off-stoichiometric lattice"¹⁴ and the liquid-like Bernal packing containing the metalloid atoms. Orientations are also of interest. Analogous to the three states of aggregation we might distinguish three states of orientation of an assembly: random orientation, preferred orientation and unique orientation (see Fig.3 bottom). Preferred orientation of an assembly is called texture, where the assembly may consist of crystals, molecules, principal axes of electric field gradients (EFG), spins etc. Texture is a common phenomenon in nature and results from processes like growth, magnetization, polarization, sedimentation, precipitation, crystallization, recrystallization, plastic deformation etc. Thus materials provided by nature or by technology are usually in the intermediate state of preferred orientations: texture. In principle, the angular dependence of the hyperfine interaction gives information on the texture of the principal axes of the electric field gradient (EFG) as well as on the texture of the spins¹⁹. However, if the magnetic interaction dominates in magnitude and a distribution of fields is present it is very difficult to evaluate any of the EFG parameters: magnitude, sign, asymmetry parameter, texture etc. In ferromagnetic materials the spin texture is of interest. In crystalline materials usually the magneto-crystalline anisotropy governs the orientations of the spins within the domains, that is, along the easy direction of magnetization. In amorphous

metals the domain patterns are determined by the three types of anisotropy energies: shape anisotropy, magnetoelastic coupling energy, and structure anisotropy²⁰. Essentially two characteristic domain patterns have been observed in amorphous metals: broad stripes with a width of about 25 μm and patches of maze or fingerprint-type patterns with a smaller domain width of about 3-5 μm . If the magnetostriction is positive²¹, as is the case for most of the amorphous $T_{80}M_{20}$ metals, the striped domain patterns can be related to regions with tensile stresses leading to easy axes within the ribbon plane, while the fingerprint domains are associated with compressive stresses producing closure domains, as for instance, shown in Fig. 4. In general,

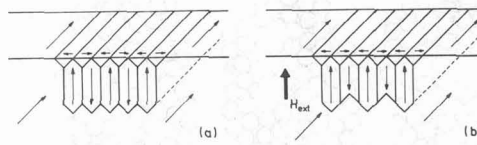


Fig.4: Suggested domain patterns metals in the crystalline state contain defects like point-, one-, two- and three-dimensional imperfections. In amorphous systems we are faced with the problem and question: do defects exist which can be described as counterparts to the known and relatively well-defined defects in the crystalline state? If amorphous metals are characterized by a breakdown of atomic order, we encounter great difficulties in imaging imperfections corresponding to such defects as vacancies, interstitials, order-disorder, dislocations, etc. For the amorphous state, most defects seem to have lost their defined meaning and structure. Let us take, as an example, dislocations, since a technologically important property of metals, plasticity, originates to a great extent in the presence and mobility of dislocations. An edge dislocation shown in Fig.5 is characterized by a

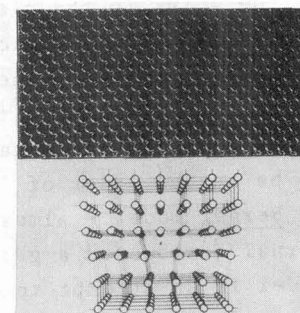


Fig.5: Edge dislocation

glide system (glide plane and glide direction) and the Burgers vector. If dislocations exist in amorphous metals the glide systems would certainly not be unique as they are for the crystalline state and the Burgers vector would be variable.

It has been shown by general continuum theory²² that internal stresses can be represented by quasi-dislocations with Burgers vectors much smaller than the distance between nearest neighbors. Kronmüller et al.²⁰ pointed out that in the rapid cooling process mass density fluctuations will occur leading to vacancy-like or interstitial-like defects. By agglomeration, zones are formed as schematically shown in Fig.6. One might consider that from an

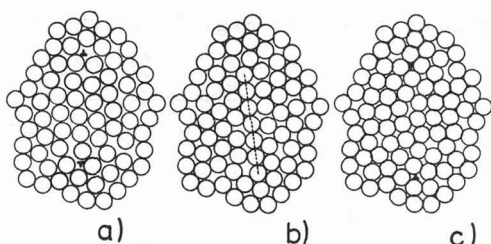


Fig.6: (b) amorphous structure forming (a) quasi-vacancy and (c) quasi-interstitial dislocations

original configuration in the center (b) seven atoms in a row have been taken out and by the local collapse most atoms do not touch each other any more as shown on the left (a). On the right a row of atoms has been added and the resulting stress is indicated by the overlap of the atoms (c). Note that the outer contours remained unchanged. The configurations in (a) and (c) with the two quasi-dislocations might be compared in three dimensions to vacancy or interstitial dislocation loops in crystalline materials. (a) leads to regions with tensile stress and preferred orientations of the spins in the plane of the ribbon, while (c) leads to regions under compression and will develop the maze type of domains. The density of these quasi-dislocations in amorphous metals were estimated²⁰ to be in the order of $10^{13}/\text{cm}^2$

4. Bernal model.- Almost two decades ago Bernal²³ proposed a general geometrical model in an attempt to explain the structure of liquids in terms of a dense random

packing (DRP) of hard spheres. The Bernal model has served in many investigations as the basis for elucidating the structure of amorphous alloys. It was noted from certain geometrical assumptions that in the DRP structure five types of polyhedra are formed. These five polyhedra were called deltahedra because of their triangular faces. They are shown in Fig. 7 with increasing

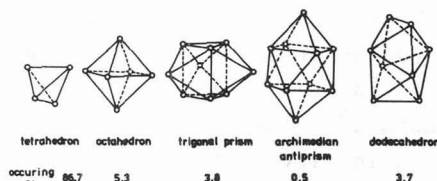


Fig.7: Holes in Bernal's DRP Topology size of the interior hole and their relative occurrence in the Bernal structure. This led Polk²⁴ to propose a model for amorphous alloys in which the larger atoms (T) form a Bernal type DRP structure while the smaller metalloïd atoms (M) are dispersed throughout. The larger polyhedra are big enough to accommodate metalloïd atoms if their atomic sizes are the same as in their crystalline states (carbides, borides, nitrides etc.). According to this model the ratio of the components for these alloys turns out to be approximately 79:21 which is close to that actually observed in amorphous metals. Bernal also investigated the number of contacts and near-contacts between each sphere and its neighboring spheres: the coordination C_0 . The relative probabilities P are given in Table 1.

Table 1

<u>Bernal</u>							
C_0	7	8	9	10	11	12	13
P	1.4	11.6	21.6	26.0	24.6	13.6	0.9
<u>Mössbauer</u>							
Int(H_1)		11.5	20.0	26.0	25.2	15.1	
H_1 (kOe)		199.2	225.5	247.7	269.4	293.9	

5. Bernal's C_0 and Mössbauer hyperfine field distributions.- Mössbauer spectroscopy allows one to probe the properties of atoms as affected by their near-neighbor arrangements. It was thought that this tool might be useful to check the validity of the Bernal model.

It is remarkable that ferromagnetic amorphous alloys with different constituents but with a composition of about $T_{80}M_{20}$ exhibit similar spectra, that is, magnetic hyperfine pattern with broad lines. The similarities suggest that it is reasonable to assume a general geometrical structure which is almost independent of the individual properties of the various constituents. In most such studies continuous hyperfine field distributions have been evaluated from the spectra. In contrast, we assumed a discontinuous distribution and decomposed the pattern into 5 subspectra²⁵ as indicated in the upper spectrum of Fig.8. It turned out that the

resulting relative intensities $Int(H_i)$ of the hyperfine fields H_i are very close to Bernal's probabilities of nearest neighbors as seen in Table 1. This suggests that the subspectra in the analysis correspond to Bernal's coordinations, C_0 (mainly 8, 9, 10, 11, 12). Accordingly, in this idealized model the hyperfine field H_i represents neighboring configurations; of course, in reality certain fluctuations, relaxations and distortions concerning the polyhedra and coordinations have to be considered, but basically each additional transition metal neighbor adds a certain amount to the field H_i . This correlation seems rather general and it holds for a large variety of ferromagnetic amorphous $T_{80}M_{20}$ alloys at various conditions of temperature, external stress and magnetic fields. Straight lines are obtained by plotting H_i versus C_0 as it

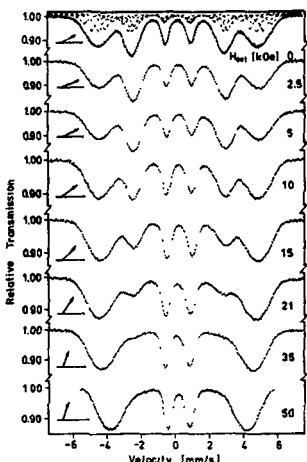


Fig. 8: $Fe_{80}B_{20}$ spectra in H_{ext} at 20 K.

Fig. 9: H_i vs. C_0

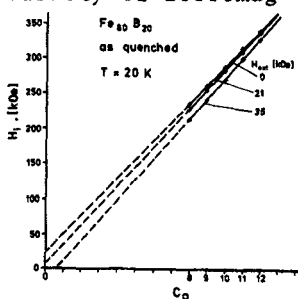


Fig. 9: H_i vs. C_0

is shown in Fig.9 for a $Fe_{80}B_{20}$ sample at 20 K and external magnetic fields, $H_{ext} = 0, 21$ and 35 kOe. Recently, this model was corroborated by Schurer and Morrish¹³.

6. Magnetic field measurements. - H_{ext} was applied perpendicular to the plane of a $Fe_{80}B_{20}$ sample and the recorded spectra²⁶ are shown in Fig.8. The following effects are of interest:

- a) Because of the negative hyperfine interaction the internal magnetic field shrinks with increasing H_{ext} .
- b) Observed asymmetries are rather small and on this basis quadrupole interactions - if they exist - could not be evaluated.
- c) Surprisingly small fields ($H_{ext} < 5$ kOe) tend to rotate the spins into the plane of the ribbon, that is away from the direction H_{ext} . The relative intensities of the lines $I_2(I_5)$ and $I_3(I_4)$ corresponding to $\Delta m=0$ and $\Delta m=\pm 1$ transitions, respectively, are given by

$$I_2/I_3 = 4 \sin^2 \theta / (1 + \cos^2 \theta),$$

and give information regarding the orientation of the spins. θ denotes the angle between the internal field and the propagation direction of the γ -rays (parallel to H_{ext}). In the case of a distribution of spin directions (domain structure) or a preferred spin orientation (spin texture) the ratio I_2/I_3 and the evaluated angle $\bar{\theta}$ represents an average. The spin directions relative to the ribbon plane are shown schematically on the left hand side of Fig.8. In Fig.10 the ratio I_2/I_3 of the as quenched and of the annealed (25 mins. at 630 K) sample is plotted versus H_{ext} . For comparison the results for a longitudinal magnetized α -Fe foil are also shown. The effect in the amorphous metals might be explained by assuming that areas of unfavorable orientations of the fingerprint domains are partly converted to stripe domains under

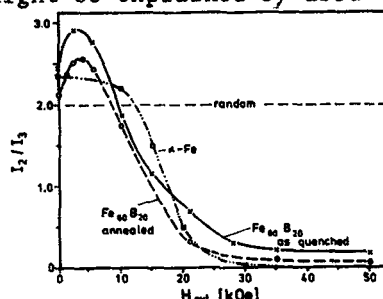


Fig. 10: I_2/I_3 vs. H_{ext}

the influence of H_{ext} as shown in Fig.4.

d) At large fields - even up to $H_{ext} = 50 \text{ kOe}$ - the $\Delta m = 0$ lines do not disappear completely ($I_2/I_3 > 0$) indicating that the saturation magnetization and complete

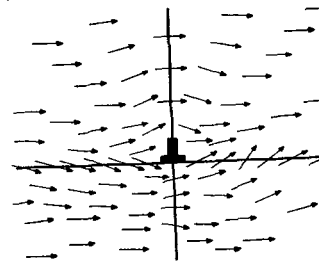


Fig.11: Spins around quasi-dislocations²⁰

alignment of the spins has not been accomplished. An explanation for this observation can be given by considering the short range (1 - 10 Å) internal elastic stresses around quasi-dislocations. This might cause an inhomogeneous spin arrangement as schematically shown in Fig.11.

7. External stress measurements. - The first measurements under stress were made unintentionally. It was observed that the magnetization vector rotates out of the plane of an amorphous ribbon when the specimen was cooled⁸. Such behavior, or the origin of the anisotropy, is difficult to understand considering the magnetic softness of the material. It was realized and demonstrated by van Diepen and den Broeder¹¹ that the cause of the rotation is basically not a thermal effect of the specimen but rather the result of the positive magnetostriction of the constrained material.

Experiments under controlled conditions were carried out by applying a tensile stress σ to the absorber ribbon ($\sigma \parallel R$) and making use of linearly polarized γ -rays²⁷. The latter were produced by a transversely magnetized source consisting of Co^{57} in α -Fe. The four $\Delta m = \pm 1$ lines are polarized perpendicular to the two $\Delta m = 0$ lines. By moving six source lines (designated by the letters A, B, C, D, E, F in ascending order of energy) over the broad absorber lines designated by the Greek letters $\alpha, \beta, \gamma, \delta, \epsilon, \eta$, we expect a 36 lines spectrum. The position of all 36 lines is easily calculated by adding or subtracting the corresponding line positions of source and absorber while the transition probabilities and

and polarizations of the corresponding transitions determine the relative line intensities. For parallel ($H_S \parallel H_A$) and perpendicular ($H_S \perp H_A$) magnetization of the source and absorber ($\text{Fe}_{40}\text{Ni}_{40}\text{P}_{14}\text{B}_6$) we expect 20 and 16 lines, respectively, which are plotted in the center part of Fig.12. For the upper spectra of Fig.12

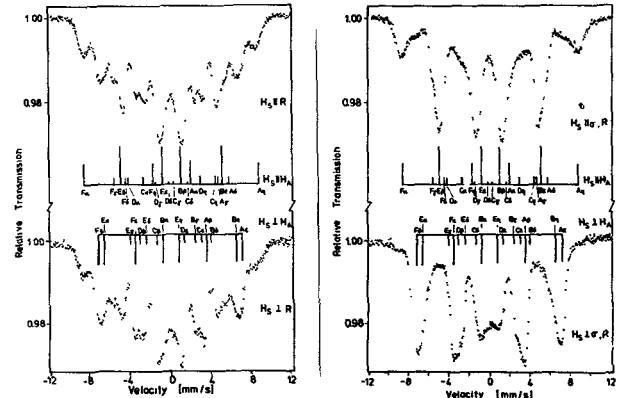


Fig.12: $\text{Fe}_{40}\text{Ni}_{40}\text{P}_{14}\text{B}_6$ spectra obtained with linearly polarized γ -rays (see text) the ribbon direction R and the source magnetic field H_S were parallel ($H_S \parallel R$) and in the lower spectra they were perpendicular ($H_S \perp R$) to each other. The two spectra on the left are rather similar, on inspection, however, differences in the relative line intensities become evident, indicating a degree of preferred orientation (texture) of the spins in the ribbon direction. By applying a tensile stress to the absorber ($\sigma \parallel R$) the spectra change considerably as shown on the right. Now the spectra for the arrangements $H_S \parallel \sigma, R$ and $H_S \perp \sigma, R$ match well with the corresponding stick diagrams indicating that the applied stress has aligned the spins.

8- Fe-Ni alloys. - The amorphous system $(\text{Fe,Ni})_{80}\text{M}_{20}$ has been studied extensively. It is interesting to compare the corresponding magnetic phase diagrams of amorphous²⁸ $(\text{Ni}_x\text{Fe}_{1-x})\text{P}_{14}\text{B}_6$ and of fcc $\text{Ni}_x\text{Fe}_{1-x}$ in the crystalline state^{29,30}. Fig.13 shows the hyperfine fields H_{int} (top) and the Curie temperature T_C and Neel temperature T_N (bottom). The T_C behaviors of the amorphous and the crystalline states are almost mirror images of each other. The high T_C values for amorphous Fe-rich

alloys indicate a large ferromagnetic Fe-Fe exchange parameter value ($J_{FeFe} = 617$ K) and a very weak Ni-Ni exchange ($J_{NiNi} \approx 0$ K)²⁸. In contrast, the high T_C values for the fcc crystalline Ni-rich alloys give evidence for a large ferromagnetic Ni-Ni exchange parameter value

($J_{NiNi} = 630$ K) and a negative - antiferromagnetic Fe-Fe exchange $J_{FeFe} \lesssim 0$ K³¹. In both cases J_{FeNi} is large. It seems that one can identify a critical concentration coinciding with the onset of either a mictomagnetic or antiferromagnetic behavior. At $0.22 \lesssim x \lesssim 0.34$ we find the invar region where coexistence of ferro- and antiferromagnetism was suggested and because of martensitic transformations it is difficult to obtain data for Fe-rich alloys ($x \lesssim 0.22$). Qualitatively one can explain the T_C behavior by considering the sensitivity of the exchange to interatomic distances as documented in the Bethe-Slater curve. With increasing distance the Fe-Fe exchange becomes positive and strongly ferromagnetic while the opposite is the case for the Ni-Ni exchange which weakens with greater atomic separation. This is what we expect in amorphous metals where the transition metal atomic distance is enlarged - compared to the crystalline alloys - by the presence of the metalloid atoms. Recently, experiments³² on amorphous $Fe_{80}B_{20}$ under tensile stress have indeed produced an increase of about 5 kOe in H_i .

II. χ -Fe

Pure χ -Fe (fcc) is unstable at room tem-

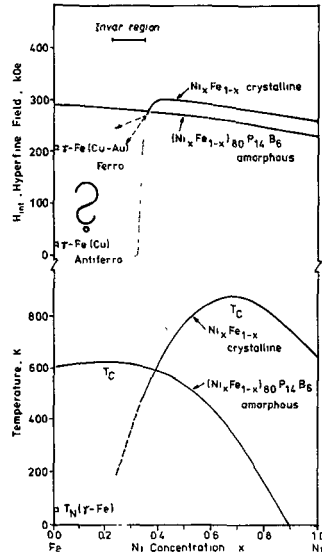


Fig. 13: H_{int} , T_C , T_N of $(Ni_xFe_{1-x})_{80}P_{14}B_6$ and fcc Ni_xFe_{1-x}

perature, but it can be stabilized by the following methods:

1. coherent precipitation in an fcc matrix, such as Cu;
2. extending the χ -phase region by alloying as, for instance, in austenitic steel;
3. producing epitaxial films on appropriate surfaces.

At the time of the discovery of the Mössbauer effect Kondorskii and Sedov³³ realized on the basis of their magnetic susceptibility measurements that antiferromagnetic ordering occurs in stainless steel at low temperature. The Néel temperatures as determined by Mössbauer spectroscopy are about 40 K for stainless steel depending somewhat on composition and 67 K for coherent fcc χ -Fe precipitates in a copper matrix³⁴. The internal field at low temperature is rather small ($H_{int} \approx 23$ kOe). Two sets of contradictory results have been obtained concerning the magnetic ordering of fcc χ -Fe films: by macroscopic methods ferromagnetism was observed in films oriented parallel to $\{111\}$ ³⁵ and $\{110\}$ ³⁶ planes. Mössbauer spectroscopy, on the other hand, established antiferromagnetism in $\{100\}$ ³⁷ films and recently also in $\{110\}$ ³⁸ films. Thus, one is tempted to conclude that the film orientation is the determining factor in the magnetic ordering. However, concurrently with the film orientation, magnetostriction produces adjustments in the lattice parameter at the coherent Cu-Fe interface. Consequently, with increasing the lattice parameter, the magnetic ordering might change from antiferromagnetic to ferromagnetic according to the Bethe-Slater curve. Recently coherent precipitates of χ -Fe produced in an expanded fcc host matrix of 69 at % Cu 30 at % Au have been found to be ferromagnetically ordered with a magnetic hyperfine field of 210 kOe³⁹. It seems that the magnetic ordering and the magnetic hyperfine field of χ -Fe films depend critically on the lattice parameter and possibly on the film orientation.

The question mark on the Fe-side in Fig. 13 should indicate that the problem concerning the magnetic stress of fcc χ -Fe has not yet been solved.

References

1. Kelly, K., Reiner, A.J., J. Irreproducible Results 24 (1978) 3
2. Buckel, W., Hilsch, R., Z. für Physik 138 (1954) 109
3. Duwez, P., Trans. Am. Soc. Metal 60 (1967) 607
4. Masumoto, T., Maddin, R., Materials Science Engineering 19 (1975) 1
5. Cargill III, G.S., in Solid State Physics, Vol. 30 (ed. H. Ehrenreich, F. Seitz and D. Turnbull) (1975) p. 227
6. Gilman, J.J., Leamy, H.J., Metallic Glasses, ASM, Metals Park Ohio
7. Tsuei, C.C., Longworth, G., Lin, S.C.H., Phys. Rev. 170 (1968) 603
8. Chien, C.L., Hasegawa, R., J. Appl. Phys. 47 (1976) 2234
9. Mangin, P., Marchal, G., Piecuch, M., Janot, Ch., J. Physique E9 (1976) 1101
10. Fujita, F.E., Masumoto, T., Kitaguchi, M., Ura, M., Jap. J. Appl. Phys. 16 (1977) 1731
11. van Diepen, A.M., den Broeder, F.J., J. Appl. Phys. 48 (1977) 3165
12. Chien, C.L., Phys. Rev. B18 (1978) 1003
13. Schurer, P.J., Morrish, A.H., Sol. State Comm. 28 (1978) 819
14. Kemeny, T. Vincze, I., Fogarassy, B., Arajs, S., Phys. Rev. B (in press)
15. Chappert, J., J. Physique C2-107 (1979)
16. Hansen, M., Anderko, K., Constitution of Binary Alloys (McGraw Hill; 1958)
17. Ostwald, W., Z. Phys. Chem. 22 (1897) 289
18. Boudreaux, D.S., Phys. Rev. B18 (1978) 4039
19. Gonser, U., Pfannes, H.-D., J. Physique C6-113 (1974)
20. Kronmüller, H., Fähnle, M., Domann, M., Grimm, H., Grimm, R., Gröger, B., J. Magn. and Magn. Mat. (in press)
21. O'Handley, R.C., Chou, C.P., J. Appl. Phys. 49 (1978) 1659
22. Kröner, E., Kontinuumstheorie der Versetzungen und Eigenspannungen (Springer-Verlag) 1958)
23. Bernal, J.D., Proc. Roy. Soc. A280 (1964) 299
24. Polk, D.E. Acta met. 20 (1972) 485
25. Gonser, U., Ghafari, M., Wagner, H.G., Proc. Int. Conf. Mössbauer Spectroscopy, Bucharest Vol. 1 (1977) 159 and J. Magn. and Magn. Mat. 8 (1978) 175
26. Wagner, H.G., Gonser, U., Schertz, A., 3. Intern. Conf. Rapidly Quenched Metals, Brighton 2 (1978) 333
27. Fischer, H., Gonser, U., Preston, R.S., Wagner, H.G., J. Magn. and Magn. Mat. 9 (1978) 336
28. Chien, C.L., Musser, D.P., Luborsky, F. E., Becker, J.J., Walter, J.L., Sol. State Comm. 24 (1977) 231
29. Gonser, U., Nasu, S., Kappes, W., J. Magn. and Magn. Mat. 10 (1979) 244
30. Johnson, C.E., Ridout, M.S., Cranshaw, T.E., Proc. Phys. Soc. 81 (1963) 1079
31. Kouvel, J.S., Magnetism and Metallurgy (ed. A.E. Berkowitz and T.E. Kneller, Academic Press, New York (1969))
32. Gonser, U., Fischer, H., Ghafari, M., Wagner, H.G., Preston, R.S., ICM München (1979)
33. Kondorskii, E.I., Sedov, V.L., Soviet Phys. JETP 8 (1959) 1104
34. Gonser, U., Meechan, C.J., Muir, A.H., Widersich, H., J. Appl. Phys. 34 (1963) 2373
35. Gradmann, U., Kümmerle, W., Tillmanns, P., Thin Solid Films 34 (1976) 249
36. Wright, J.G., Phil. Mag. 24 (1971) 217
37. Keune, W., Halbauer, R., Gonser, U., Lauer, J., Williamson, D.L., J. Appl. Phys. 48 (1977) 2976
38. Halbauer, R., Gonser, U., (to be published)
39. Gonser, U., Krischel, K., Nasu, S., ICM München (1979)